Vrije Universiteit Brussel

Microfluidic Device for High-Throughput Production of Monodisperse Droplets

Gelin, Pierre Philippe; Bihi, Ilyesse; Ziemecka, Iwona; Thienpont, Benoit; Christiaens, Jo Wim; Hellemans, Karine H; Maes, Dominique; De Malsche, Wim

Published in:
Industrial & Engineering Chemistry Research

DOI:
10.1021/acs.iecr.9b05935

Publication date:
2020

Document Version:
Accepted author manuscript

Link to publication

Citation for published version (APA):
Gelin, P. P., Bihi, I., Ziemecka, I., Thienpont, B., Christiaens, J. W., Hellemans, K. H., Maes, D., & De Malsche, W. (2020). Microfluidic Device for High-Throughput Production of Monodisperse Droplets. *Industrial & Engineering Chemistry Research*, *59*(28), 1-7. [ie-2019-05935r.R2]. https://doi.org/10.1021/acs.iecr.9b05935

Copyright
No part of this publication may be reproduced or transmitted in any form, without the prior written permission of the author(s) or other rights holders to whom publication rights have been transferred, unless permitted by a license attached to the publication (a Creative Commons license or other), or unless exceptions to copyright law apply.

Take down policy
If you believe that this document infringes your copyright or other rights, please contact openaccess@vub.be, with details of the nature of the infringement. We will investigate the claim and if justified, we will take the appropriate steps.

Download date: 03. Apr. 2024

Microfluidic device for high throughput production of monodisperse droplets

*Pierre Gelin[§], Ilyesse Bihi[§], Iwona Ziemecka[§], Benoit Thienpont[§], Jo Christiaens[§], Karine Hellemans[‡], Dominique Maes[†], Wim De Malsche[§]**

[§] μFlow group, Department of Bioengineering Sciences, Department of Chemical Engineering, Vrije Universiteit Brussel, 1050 Brussels, Belgium.

[†]Structural Biology Brussels, Vrije Universiteit Brussel, 1050 Brussels, Belgium.

[‡] Unit Diabetes Pathology and Therapy, Diabetes Research Center, Vrije Universiteit Brussel, 1000 Brussels, Belgium

ABSTRACT

In this study we present a novel microfluidic device for high throughput production of monodisperse droplets. The proposed 3D-emulsifier consists of multiple parallel droplet generators coupled to only two inlets (continuous and dispersed phase). The three-dimensional nature of our device allows for a maximal density of droplet generators per surface area. We produce oil droplets in water using a device containing a single and four droplet generators. The droplet size and throughput were experimentally determined. In the four nozzle chip, we observe an important effect of the flow rate on the size distribution between the different droplet generators. Importantly, the transition between the squeezing and a transition regime shows the highest monodispersed production rate. For the four nozzle chip, we show a four-fold increase of the production throughput, while maintaining a high monodispersity of the droplets. A theoretical scale-up of our device is performed, demonstrating a possible throughput of 8.2 l/h, opening the door for (industrial) applications requiring much larger flow rates than what is typically achievable with microfluidic devices.

1. INTRODUCTION

Microfluidic devices have been introduced more than 20 years ago and were believed to induce breakthroughs in society and industry due to the conceptual advantages related to flow control and the possible integration of a wide range of functionalities. Droplet microfluidics encompassing droplet formation allows for the production of highly uniform micro and nano-emulsions, which is not achievable with conventional macroscopic techniques. Uniform emulsions find a wide range of application in the pharmaceutical[1], food[2] and chemical industry[3], offering e.g. a better drug

release, stability or yield. However, the low production rate of microfluidic devices remains one of the main bottlenecks for their use in industrial applications. Production rates exceeding 1 l/h are commonly needed. In typical one droplet generation systems, the frequency of droplet generation can reach 1000 to 12 000 Hz, the volume at these frequencies remain low (2.8 ml/h for 50 µm droplets)[4]. Recent research in microfluidics has, however, focused on making the flow rates obtained with microfluidics sufficiently large for industrial applications. To this end, novel chip configurations with multiple droplet generators have been proposed, including: (i) step emulsifiers and parallelized microfluidic droplet generators. (i) Step emulsification relies on distributing the dispersed phase through discrete channels, forming droplets in the surrounding continuous phase. In these type of devices, droplets are formed spontaneously due to static instabilities, leading to highly monodispersed droplets[5–10]. However, droplet size cannot be varied as it is solely dependent on the device geometry. A disadvantage of these type of micro arrays is a limited droplet production due to its 2D nature[11]. Amstad *et al.* fabricated a microfluidic chip containing 500 droplet generators, reaching a throughput of 150 ml/h[10]. To address the relatively low throughput of in-plane step emulsifiers, vertical channels were introduced[12–16]. Using this design Stolovicki *et al*. have reported a maximal throughput of 10 l/h in a device including 120 througholes[15]. (ii) In contrast to spontaneous drop generation, multiple designs exist which aim to parallelize classical droplet generators (T-nozzles and flow focusing). Droplet formation in these devices is largely controlled by the flow rates of the dispersed and continuous phases, allowing to vary the droplet size easily. Nisisako and coworkers reported on a device containing 256 flow focusing droplet generators arranged in a circular configuration. The authors reported a throughput of 320 ml/h[17]. Two common layouts exist to distribute the liquids, the tree distributor and the ladder distributor[11]. Tree-like emulsifiers rely on bifurcating a single channel into 2^N daughter channels over N

generations[18–20]. Using this strategy, Conchouso *et al.* have reported a circular array comprising 128 flow focusing droplet generators, allowing for a production rate of 1 l/h[19]. Ladder-like emulsifiers are more commonly used[21–27], these distribute liquids through small channels, characterized by a high flow resistance, which are directly connected to a main 'backbone' channel[11]. Romanowsky *et al*. developed a microfluidic device comprised of 15 flow focusing devices for the production of double emulsions[26]. The authors demonstrated a possible throughput of 42 ml/h. Similarly Yadavali *et al*., incorporated 10260 droplet generators on a microfluidic chip for a total production rate of 2.09 l/h[27].

While great progress has already been achieved in the parallelization of microfluidic droplet generators, there is still room for improvement. The above reported devices produce droplets in the two-dimensional plane. This allows a nice visualization of the droplet formation but limits the nozzle density and makes coupling to larger scale reactors difficult. To the best of our knowledge only one truly 3D design has been reported, which is based on the ladder-like distributors[28]. However, the droplet generators are on a single line, again limiting the density of droplet generators. In this paper we propose a novel approach for the high throughput production of monodispersed droplets with a polydispersity on the order of 5%. Our device is designed in such a way that the droplet generators are perpendicular to the distribution planes. This configuration allows for a maximal nozzle density on a given surface. To the best of our knowledge this full three-dimensional emulsifier has never been demonstrated before. To validate our device oil droplets are produced in water. Moreover, a theoretical upscaling exercise of our concept is worked out and compared to state of the art approaches, taking pressure limitations into account.

2. EXPERIMENTAL

2.1. Chip design and fabrication. The 3D emulsifier is designed such that the first and second dimension are used for flow distribution. Flow distribution is based on ramified or tree-like distributors, originally introduced and characterized by Tondeur and Luo[29,30]. The ramified distributor consists of channels that are sequentially bifurcating in two 'daughter' channels, forming different generations. Droplets are formed perpendicular to the distribution plane, these sites of droplet generation can be seen as 2D T-nozzles equivalents in 3 dimensional space. While flow focusing nozzle can also be envisaged, the current study is limited to the use of the T-nozzle contact type, which produces a more controllable droplet generation and has higher tolerance for flow irregularities with limited impact on the droplet size distribution[31]. A distributor of N generations has 2^N droplet generators. This exponential increase in droplet generators with each generation, allows to easily design a device with a multitude of droplet generators.

The 3-D emulsifier comprises three separate layers. Two layers for the distribution of the continuous and dispersed phase, respectively, and a cover lid (Figure 1.a). The distribution channels for the continuous phase have a width of 1000 μm and a depth of 200 μm, except for the final branch which has a width of 200 μm. The distributor for the dispersed phase has channels with a width and depth of 1000 μm. Each droplet generator consists of two concentric holes, one connecting the discrete phase with the continuous phase and a second acting as an outlet. Both holes have a diameter of 150 μm and 300 μm, respectively. To ensure good flow distribution in the chip, the final part of the distributor, before the droplet generator, is designed such that it experiences the highest pressure drop in comparison with the rest of the distributor[26]. For the continuous phase distributor this high pressure drop part corresponds to the final branch of the

ramified distributor. For the dispersed phase, however, the highest pressure drop is achieved in the hole located just before the junction (Figure 1.a; enlargement).

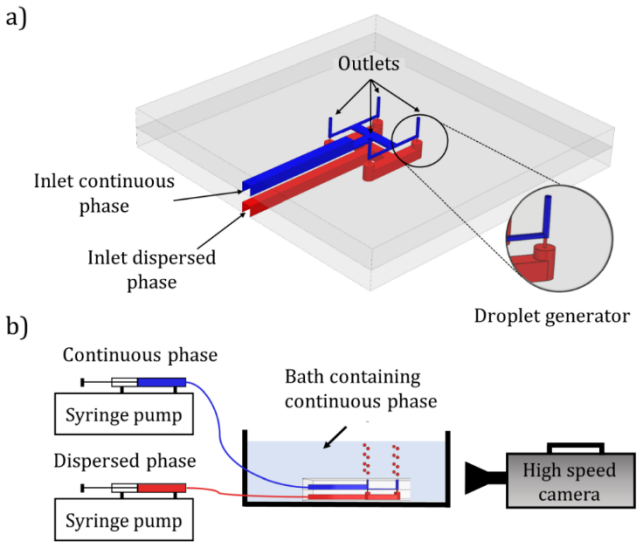

Figure 1. a) Overall view of the 3D-emulsifier containing four nozzles and a magnification of a droplet generator (see inset for detail). Each layer comprises a distributor connected via through holes. These form the location for droplet formation. The lid sealing the device is not shown in the representation. b) Schematic representation of the setup. Two syringe pumps supply the continuous and dispersed phase to the 3D-emulsifier. The emulsifier was positioned in a recipient containing the continuous phase. Droplet formation was recorded with a high speed camera.

The 3-D emulsifier was fabricated in polymethyl-methacrylate (PMMA), this polymer was chosen for its transparency, chemical resistivity and ease of micromachining. A high speed CNC milling machine (Datron Neo, Datron AG., Germany) was used to mill the microfluidic channels. The three different layers were subsequently assembled. First, all layers were rinsed with isopropyl alcohol then dried with an air gun. Sealing of the chip was achieved by solvent assisted bonding of the three substrates. Two clean PMMA layers were positioned and aligned prior to bonding. Less than 5 µl butyl lactate was injected using a pipette at the edge between the PMMA pieces.

Due to capillary forces, butyl lactate flowed into the interstitial space without overflowing into the channels. Then, the two pieces were allowed to bond without additional pressure at room temperature for at least three hours. Finally, the same process was repeated to bond the third layer. Two versions of the 3D-emulsifier were produced. One containing a single droplet generator, to validate the formation of monodisperse droplets in the proposed geometry and serving as reference for the second version which contains 4 droplet generators.

2.2. Experimental setup. A schematic representation of the setup is shown in Figure 1.b. The continuous phase consists of water containing polyvinyl alcohol, PVA (2 wt%, 9-10 kDa, 80% hydrolyzed, Sigma-Aldrich) as a surfactant, hexane (VWR chemicals) containing Span 80 (20 wt%, Merck) was chosen as the dispersed phase. The viscosity of the continuous and dispersed phase was measured to be $1.6*10^{-3}$ Pa*s ± $8.1*10^{-5}$ and $5.3*10^{-4}$ Pa*s ± $2.1*10^{-5}$, respectively. Liquids are fed into the 3D-emulsifier by two syringe pumps (KDS 100, KD Scientific, USA), through fused-silica capillaries. The emulsifier itself was submerged into a bath containing the continuous phase. For all experiments, a constant flow ratio of 1:1 of the continuous and dispersed phase was maintained ($Q_{water} = Q_{hexane}$). Droplet formation was recorded with a CMOS high speed camera (pco.dimax HS4, PCO AG, Germany). The obtained movies were further analyzed using MATLAB and ImageJ.

3. RESULTS AND DISCUSSION

3.1. Droplet formation. Both 3D-emulsifiers were evaluated by forming hexane droplets in water. The flow rate ratio was kept constant at a ratio of 1:1 ($Q_{water} = Q_{hexane}$). The emulsifier containing a single nozzle was first used to characterize the droplet formation regimes. Three

different regimes were observed, the squeezing regime, a transition regime and finally the jetting regime. To distinguish the transition between the observed regimes, the length of the neck right before break-up was measured and normalized by the diameter of the outlet nozzle (D = 300 µm). Figure 2 depicts the evolution of the normalized break-up length (L_D/D) with the applied flow rate. The increase of the break-up length with the flow rate can be clearly seen. The threshold value selected for the squeezing regime transition is $L_D/D = 1$[32–35]. Droplets with a low break-up length ($L_D/D < 1$) were considered to be generated in the squeezing regime. This cut off is equivalent to a flow rate of 4.5 ml/h/nozzle. Above a flow rate of 9 ml/h/nozzle, a well-developed jet is observed with clear instabilities.

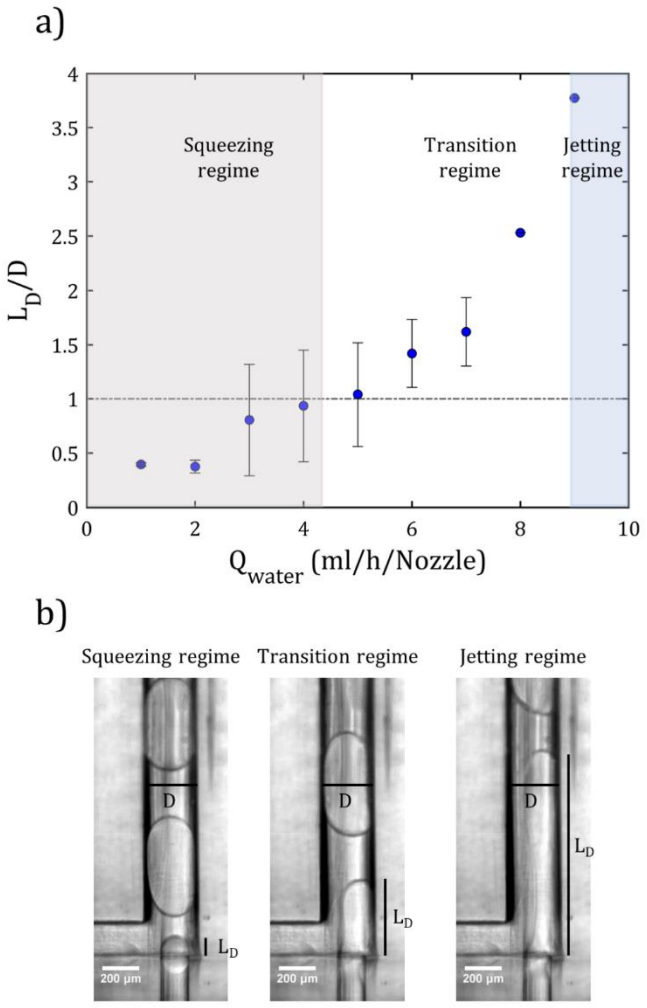

Figure 2. a) Normalized break-up length (L_D/D) at different flow rates. Three droplet formation regimes are identified: (i) the squeezing regime, (ii) a transition regime and (iii) the jetting regime. The dotted line represents the transition from the squeezing regime to the jetting regime ($L_D/D > 1$). b) Photographs of droplet formation at the moment of break-up in the three different regimes.

Since in the present study the interest lies in the formation of monodispersed droplets, all our next experiments were conducted at flow rates were the squeezing regime or transition regime dominates. The droplet sizes and the throughput at different flow rates are shown in Figure 3. At flow rates below 4.5 ml/h/nozzle a relatively constant droplet size is observed with an average volume of $9.1*10^6$ µm³ ± $0.4*10^6$. At flow rates above 4.5 ml/h/nozzle, the droplet volume drops

to $7.7*10^6$ µm³ ± $0.2*10^6$. This difference in droplet size can be explained by the transition from the squeezing regime to the transition regime at a flow rate of 4.5 ml/h/nozzle. This is consistent with the previous study of the break-up length and the used threshold of $L_D/D = 1$. The relatively constant droplet size in both regimes, indicates that our system is stable across a range of flow rates for the production of highly uniform particles. Figure 3 depicts also a linear rise of the throughput (droplets/s) with the applied flow rate. It should be noted that at the edge between the squeezing and transition regime the formed droplets show a slightly higher variance.

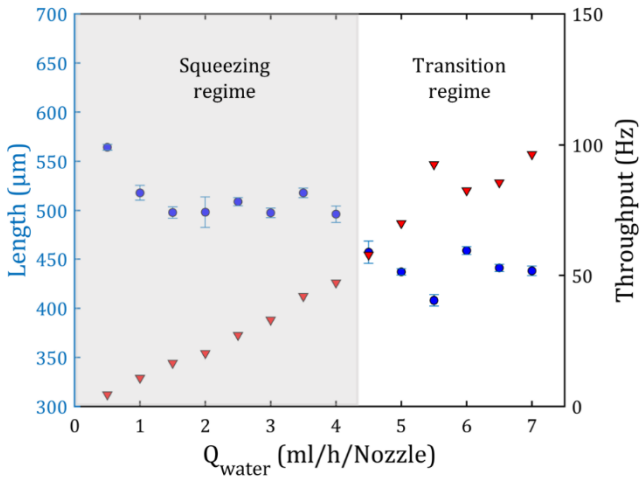

Figure 3. Droplet length (●) (left y-axis) and throughput (▼) (right y-axis) as a function of the applied water flow rate. Two distinct break-up regimes are observed (the squeezing and a transition regime), with a transition around 4.5 ml/h/nozzle. The pictures show the squeezing regime at a flow rate of 2.5 ml/h/nozzle and the transition regime at a flow rate of 6 ml/h/nozzle.

Droplet formation inside the four nozzle chip is shown in Figure 4. At flow rates of 1-4 ml/h/nozzle the squeezing regime dominates inside the nozzle. Figure 4.b and 4.c show monodisperse droplets exiting the 3D-emulsifier.

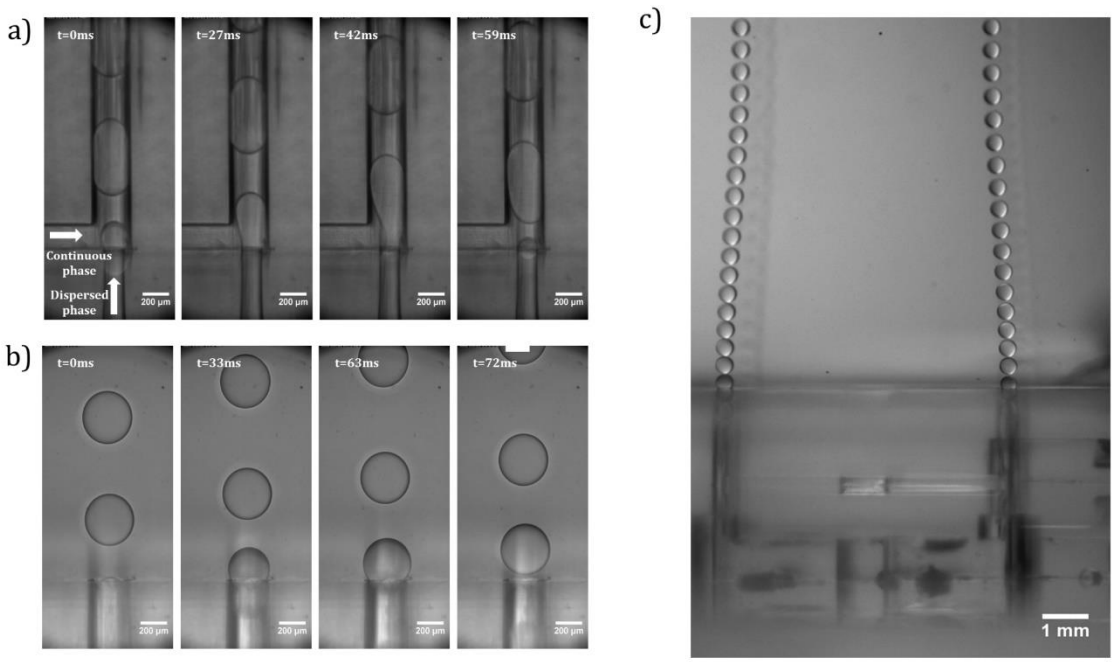

Figure 4. Time-lapse of droplet formation a) inside the 3D-emulsifier and b) outside the 3D-emulsifier. The flow rate of the continuous and dispersed phase was set at 1 ml/h/nozzle. c) Overview image of a 4 nozzle 3D-emulsifier producing hexane droplets at a flow rate of 4 ml/h/nozzle. Only two nozzles are visible, the others are out of focus.

The device which contains 4 nozzles does not show a constant but a decreasing droplet size with rising flow rate. Only at a higher flow rate a size similar to the one nozzle chip was observed (Figure 5.a). Moreover, the coefficient of variance (CV) decreases with rising flow rate, until a flow rate of 4 ml/h/nozzle, after which it rises again (Figure 5.b). It should be noted, that when looking at individual nozzles within the 4-nozzle design, monodispersed droplets are formed. The measured variability on the droplet size is, as a consequence, the result of size variation between the different nozzles and not of variations at single nozzle level. Droplet formation is a fine interplay between interfacial phenomena and dynamical ones. At low flow rates, the interfacial phenomena dominate and the droplet formation process can be seen as minimization of the

interfacial energy. At these flow rates the continuous phase cannot overcome the interfacial tension during droplet formation at a certain outlet. Hence the pressure drop of the continuous phase rises localy[36]. This deviates the continuous phase to another outlet, delaying the pinch-off of the droplet. Thus the high CV at low flow rates could be explained by communication between the droplet generators. This phenomenon could also be seen from a perspective of minimizing the interfacial energy, hence at very low rates (smaller than the studied range), dispersed phase will fill one or two nozzles, and the continuous phase will fill the two others. Thus very huge droplets will come out from the first 2 nozzles and no droplets will come out from the other nozzles. At a flow rate of 4 ml/h/nozzle, this phenomenon seems to be less pronounced leading to more uniform droplets. At flow rates higher than 4 ml/h/nozzle, some nozzles shift into the transition regime while others remain in the squeezing regime. Because the transition regime generates smaller droplets than the squeezing regime (Figure 3), this shift is associated with a rise in CV.

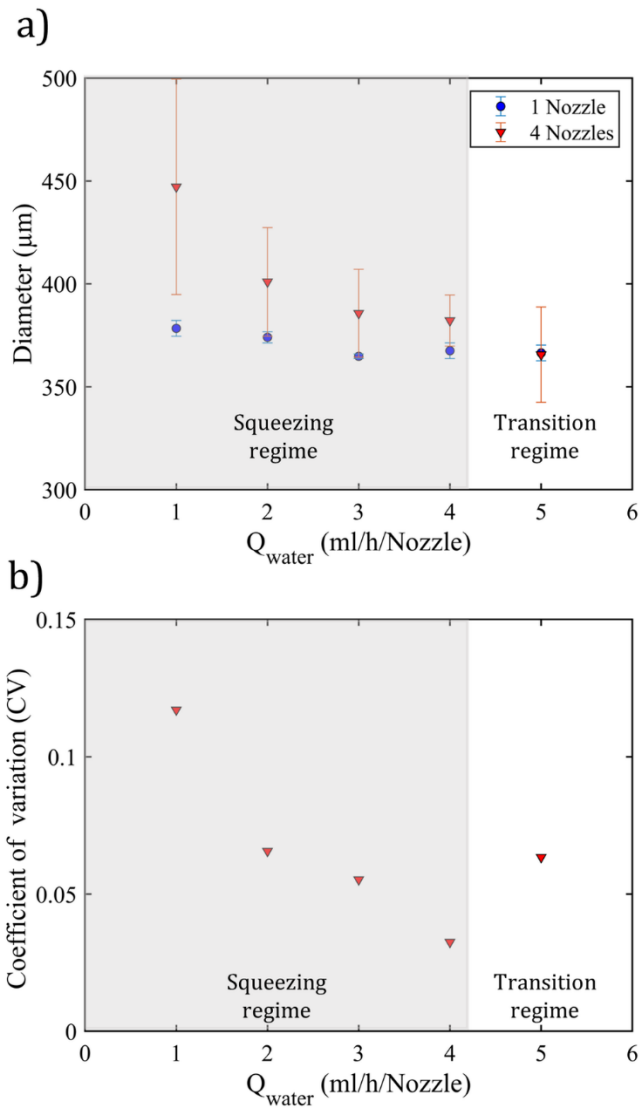

Figure 5. a) Measured droplet diameter as a function of flow rate for chips containing one (●) or four (▼) nozzles. b) Coefficient of variance of the droplet size for an emulsifier containing four nozzles. At a flow rate larger than 4 ml/h/nozzle a transition from the squeezing regime to the transition regime occurs, explaining the higher CV.

The frequency of droplet generation rises linearly for a single nozzle emulsifier (Figure 6). This is expected since the droplet size remains constant. A maximal throughput of 53 Hz is observed at a flow rate of 5 ml/h/nozzle. As one would expect, the total throughput is higher for the four nozzle

3D-emulsifier (see inset). At a flow rate of 4 ml/h/nozzles, which gave equal droplet size in the 1 and 4 nozzle 3D-emulsifier, the expected four-fold increase in throughput is observed. At lower flow rates, larger droplets are formed and thus the throughput (in terms of droplet frequency) is slightly lower.

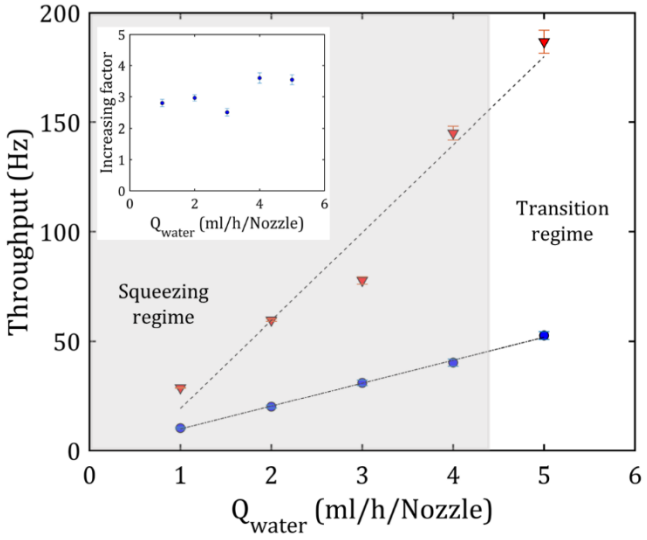

Figure 6. Frequency of droplet generation as a function of flow rate per nozzle for an emulsifier containing one nozzle (●) or four nozzles (▼). A fourfold increase in throughput is observed at a flow rate of 4 ml/h/nozzle when going from one nozzle to four nozzles (inset). The dotted lines show the expected linearity of the throughput in function of the applied flow rates.

3.2 Design rules for upscaling. For our 3D emulsifier, a couple of design rules needs to be undertaken, especially when thinking of upscaling the device with thousands of droplet generators with a high density. The first rule is ensuring a minimal pressure drop, such that a syringe pump can be used ($\Delta P < 2$bar). The second one is to ensure a uniform flow across each droplet generator, even if some of the nozzles are clogged. Applying Ohm's law and Kirchhoff's law to the equivalent electric circuit to our system represented in Figure 7.a, yields the following relationships[37,38]:

$$-\Delta P_d = R_{d0}Q_d + \sum_{i=1}^{N} R_{d1i}Q_{di} + R_2Q_{out} + \rho gz \quad [1]$$

$$-\Delta P_c = R_{c0}Q_c + \sum_{i=1}^{N} R_{c1i}Q_{ci} + R_2Q_{out} + \rho gz \quad [2]$$

where ΔP_d and ΔP_c are the pressure differences of the dispersed and the continuous phases, respectively. R_{d0} and R_{c0} are the hydraulic resistances of the capillary tubes transporting the liquids into the microfluidic chip. After entering the device, the liquids are distributed over the branches. In each branch "i", R_{d1i} , Q_{di} and R_{c1i} , Q_{ci} represent the hydraulic resistance and the flow rate of the dispersed and the continuous phase. At the end of the two distributors, the liquids meet at the droplet generator. Droplets are formed at the last channel that has a resistance R_2. Finally, the droplets are released in the reservoir. An additional pressure is then added that depends on the level of water, z, in the reservoir. It should be noted that the objective of this calculation is to have an order of magnitude of the pressure drop through the system. Accurate calculation of the pressure drop is out of the scope of this study. In our experiments the overall pressure drop does not exceed 0.1bar. This low pressure drop allows the use of simple equipment like low pressure or syringe pumps.

To ensure the production of highly monodisperse droplets, proper distribution of the continuous and dispersed phase is crucial. To this end, the guidelines proposed by Tondeur and Luo[29] for the design of a ramified distributor have been adapted such that the final branch is much smaller than the other branches. This introduces a high flow resistance in the final part of the distributor. As a result, the quality of flow distribution is only influenced to a minor extent by small fabrication deviations (or fouling) at the upstream zone of the distributor. Figure 7.b depicts the pressure drop in a 4 nozzle 3D-emulsifier, for the distribution of the continuous and the dispersed phase. The inlet flow rate of both phases was assumed to be 5 ml/h/nozzle. Each generation of the distributors

is denoted by a letter (A-D). Note that the distributor of the dispersed phase has as additional generation compared to the continuous phase. This final level corresponds to the hole connecting the two distributors (see inset at Figure 1.a). The blue squares denote the location of the junction where the dispersed and continuous phase meet. We observe a sharp rise in pressure drop at the final branch of each distributor as required by the design rule.

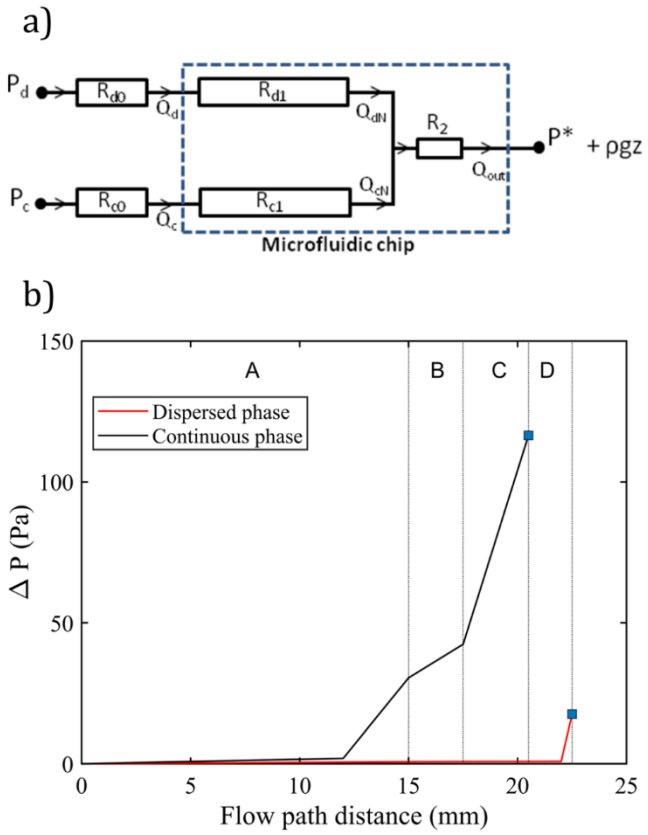

Figure 7. a) Schematic representation of the experimental setup as an electrical circuit. b) Pressure drop in a 4 nozzle 3D-emulsifier for the continuous phase (black) and the dispersed phase (red). The inlet flow for both phases is assumed to be 5 ml/h/nozzle. The blue square denotes the position where the continuous and dispersed phase meet to form a droplet.

3.3 Theoretical upscaling. Based on the obtained results in section 3.1, we performed a theoretical scale-up of our 3D-emulsifier. A throughput of 4 ml/h/nozzle was assumed since this

gave comparable droplets to our 1 nozzle benchmark. Note that for each new generation the number of nozzles rises exponential with a power of 2. As a result, the total throughput also rises exponentially. For a chip containing 2048 nozzles a theoretical total throughput of 8.2 l/h can potentially be achieved (Figure 8.a). Next to the throughput, the maximal amount of nozzles that can be implemented on a chip with a size of 1 cm² is calculated. Defining the width of the inlet channel as w_1 and the final channel as w_N, the maximal number of nozzles can be calculated from[29]:

$$\left(\frac{w_1}{2}+\frac{w_N}{2}\right)*2^{1+\frac{N}{2}}<\sqrt{A} \qquad [3]$$

with N the number of generations. In our scale-up the width of the first and last channel was assumed to be 200 µm, as this is the minimal achievable channel size using our milling machine. The through holes were kept at a diameter of 300 µm. With these boundary conditions, a total number of 256 nozzles could be implemented on a 1 cm² chip (Figure 8.b). Note that, the requirement of the sharp rise in pressure drop in the final branch of the distributor, can be maintained by varying the channel heights. When using higher resolution fabrication methods based on lithography and etching, or alternatively laser ablation, much smaller sizes and thus higher nozzle densities could be achieved in a 3D emulsifier configuration. As an example, for channel sizes of 100 µm a total of 2048 nozzles could be implemented on a 1 cm² chip. This would correspond to a total flow rate of 8.2 l/h. This nozzle density on a surface of only 1 cm² is unprecedented and has become possible because of the full 3D nozzle configuration. The experimental development of a high density 3D-emulsifier will be performed in a follow-up study. Based on the presented results, scale-up of our 3D-emulsifier seems to be a highly promising for high throughput production in industrial applications.

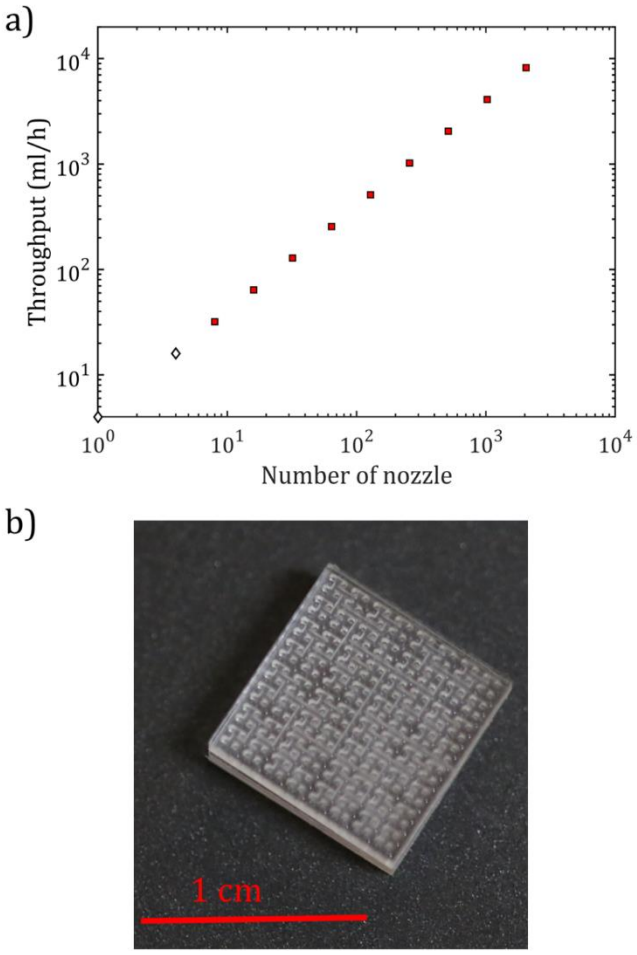

Figure 8. a) Theoretical scale-up of current 3D-emulsifier, assuming a throughput of 4 ml/h/nozzle up to 2048 nozzles. Experimental throughput (◇) and theoretical throughput (■). b) Photograph of a 1cm² 3D-emulsifier containing 256 nozzles.

4. CONCLUSION

We have introduced a novel microfluidic device, specifically designed for high throughput production of microdroplets and microparticles. The 3D-emulsifier is designed such that the droplet generators are perpendicular to the distribution planes, allowing for a maximal nozzle density. The droplet size and throughput were measured in a one and four nozzle design. In the four nozzle device, an optimal flow rate of 4ml/h/nozzle was observed at which monodispersed

droplets (370 µm ± 6.4) were formed in all droplet generators. This flow rate corresponds to the switch between the squeezing and a transition regime. Moreover, a four-fold increase was observed in the throughput for the four nozzle 3D-emulsifier. To ensure an appropriate flow distribution of the liquids, the final part of the distributor was design such that it has the highest pressure drop compared to the upstream part of the emulsifier. While the current 3-D emulsifier only had 4 nozzles, a theoretical scale-up under realistic conditions has been demonstrated. Expanding our design to a 1 cm² chip containing 2048 nozzles could give a throughput of 8.2 l/h. This is a significant increase compared to other nozzle array devices described in literature, paving the way for use of nozzle arrays in (industrial) processes requiring large throughput.

ASSOCIATED CONTENT

Supporting Information. Video S1, Droplet formation inside the droplet generator, Video S2, Droplet coming out of 3D-emulsifier, Video S3, Enlarged view of the droplet formation in the 4 nozzle 3D-emulsifier.

AUTHOR INFORMATION

Corresponding Author

E-mail: wim.de.malsche@vub.be; Tel: +32 2 629 37 81

Author Contributions

The manuscript was written through contributions of all authors. All authors have given approval to the final version of the manuscript.

ACKNOWLEDGMENT. Wim De Malsche and Pierre Gelin greatly acknowledge the European Research Council for support through ERC starting Grant EVODIS (grant number 679033EVODIS ERC-2015-STG). Ilyesse Bihi acknowledges Innoviris for financial support (Evaluate grant ‘Microdrop’). The authors greatly acknowledge Joost Brancart for his measurements of the viscosity of the liquids.

REFERENCES

(1) Rezvantalab, S.; Keshavarz Moraveji, M. Microfluidic Assisted Synthesis of PLGA Drug Delivery Systems. *RSC Adv.* **2019**, *9* (4), 2055–2072. https://doi.org/10.1039/C8RA08972H.

(2) Neethirajan, S.; Kobayashi, I.; Nakajima, M.; Wu, D.; Lin, F. Microfluidics for Food, Agriculture and Biosystems Industries. *Lab Chip* **2011**, *11*, 1574–1586. https://doi.org/10.1039/c0lc00230e.

(3) Elvira, K. S.; I Solvas, X. C.; Wootton, R. C. R.; Demello, A. J. The Past, Present and Potential for Microfluidic Reactor Technology in Chemical Synthesis. *Nat. Chem.* **2013**, *5* (11), 905–915. https://doi.org/10.1038/nchem.1753.

(4) Yobas, L.; Martens, S.; Ong, W. L.; Ranganathan, N. High-Performance Flow-Focusing Geometry for Spontaneous Generation of Monodispersed Droplets. *Lab Chip* **2006**, *6* (8), 1073–1079. https://doi.org/10.1039/b602240e.

(5) Sugiura, S.; Nakajima, M.; Itou, H.; Seki, M. Synthesis of Polymeric Microspheres with Narrow Size Distributions Employing Microchannel Emulsification. *Macromol. Rapid Commun.* **2001**, *22* (10), 773–778. https://doi.org/10.1002/1521-3927(20010701)22:10<773::AID-MARC773>3.0.CO;2-H.

(6) Sugiura, S.; Nakajima, M.; Tong, J.; Nabetani, H.; Seki, M. Preparation of Monodispersed Solid Lipid Microspheres Using a Microchannel Emulsification Technique. *J. Colloid Interface Sci.* **2000**, *227* (1), 95–103. https://doi.org/10.1006/jcis.2000.6843.

(7) Kobayashi, I.; Wada, Y.; Uemura, K.; Nakajima, M. Microchannel Emulsification for Mass

Production of Uniform Fine Droplets: Integration of Microchannel Arrays on a Chip. *Microfluid. Nanofluidics* **2010**, *8* (2), 255–262. https://doi.org/10.1007/s10404-009-0501-y.

(8) Kawakatsu, T.; Trägårdh, G.; Kikuchi, Y.; Nakajima, M.; Komori, H.; Yonemoto, T. Effect of Microchannel Structure on Droplet Size during Crossflow Microchannel Emulsification. *J. Surfactants Deterg.* **2000**, *3* (3), 295–302. https://doi.org/10.1007/s11743-000-0132-1.

(9) Ofner, A.; Moore, D. G.; Rühs, P. A.; Schwendimann, P.; Eggersdorfer, M.; Amstad, E.; Weitz, D. A.; Studart, A. R. High-Throughput Step Emulsification for the Production of Functional Materials Using a Glass Microfluidic Device. *Macromol. Chem. Phys.* **2016**, *201600472*, 1600472. https://doi.org/10.1002/macp.201600472.

(10) Amstad, E.; Chemama, M.; Eggersdorfer, M.; Arriaga, L. R.; Brenner, M. P.; Weitz, D. A. Robust Scalable High Throughput Production of Monodisperse Drops. *Lab Chip* **2016**, *16* (21), 138–155. https://doi.org/10.1039/C6LC01075J.

(11) Vladisavljević, G. T.; Khalid, N.; Neves, M. A.; Kuroiwa, T.; Nakajima, M.; Uemura, K.; Ichikawa, S.; Kobayashi, I. Industrial Lab-on-a-Chip: Design, Applications and Scale-up for Drug Discovery and Delivery. *Adv. Drug Deliv. Rev.* **2013**, *65* (11–12), 1626–1663. https://doi.org/10.1016/j.addr.2013.07.017.

(12) Kobayashi, I.; Mukataka, S.; Nakajima, M. Novel Asymmetric Through-Hole Array Microfabricated on a Silicon Plate for Formulating Monodisperse Emulsions. *Langmuir* **2005**, *21* (17), 7629–7632. https://doi.org/10.1021/la050915x.

(13) Vladisavljević, G. T.; Kobayashi, I.; Nakajima, M. Generation of Highly Uniform Droplets

Using Asymmetric Microchannels Fabricated on a Single Crystal Silicon Plate: Effect of Emulsifier and Oil Types. *Powder Technol.* **2008**, *183* (1), 37–45. https://doi.org/10.1016/j.powtec.2007.11.023.

(14) Kobayashi, I.; Takano, T.; Maeda, R.; Wada, Y.; Uemura, K.; Nakajima, M. Straight-through Microchannel Devices for Generating Monodisperse Emulsion Droplets Several Microns in Size. *Microfluid. Nanofluidics* **2008**, *4* (3), 167–177. https://doi.org/10.1007/s10404-007-0167-2.

(15) Stolovicki, E.; Ziblat, R.; Weitz, D. A. Throughput Enhancement of Parallel Step Emulsifier Devices by Shear-Free and Efficient Nozzle Clearance. *Lab Chip* **2017**, *18* (1), 132–138. https://doi.org/10.1039/c7lc01037k.

(16) Kobayashi, I.; Neves, M. A.; Wada, Y.; Uemura, K.; Nakajima, M. Large Microchannel Emulsification Device for Mass Producing Uniformly Sized Droplets on a Liter per Hour Scale. *Green Process. Synth.* **2012**, *1* (4), 353–362. https://doi.org/10.1515/gps-2012-0023.

(17) Nisisako, T.; Torii, T. Microfluidic Large-Scale Integration on a Chip for Mass Production of Monodisperse Droplets and Particles. *Lab Chip* **2008**, *8* (2), 287–293. https://doi.org/10.1039/b713141k.

(18) Li, W.; Greener, J.; Voicu, D.; Kumacheva, E. Multiple Modular Microfluidic (M3) Reactors for the Synthesis of Polymer Particles. *Lab Chip* **2009**, *9* (18), 2715–2721. https://doi.org/10.1039/b906626h.

(19) Conchouso, D.; Castro, D.; Khan, S. a; Foulds, I. G. Three-Dimensional Parallelization of Microfluidic Droplet Generators for a Litre per Hour Volume Production of Single

Emulsions. *Lab Chip* **2014**, *14* (16), 3011–3020. https://doi.org/10.1039/c4lc00379a.

(20) Kang, D.-K.; Gong, X.; Cho, S.; Kim, J.-Y.; Edel, J. B.; Chang, S.-I.; Choo, J.; Demello, A. J. 3D Droplet Microfluidic Systems for High-Throughput Biological Experimentation. *Anal. Chem.* **2015**, *87*, 10770–10778. https://doi.org/10.1021/acs.analchem.5b02402.

(21) Tetradis-Meris, G.; Rossetti, D.; De Torres, C. P.; Cao, R.; Lian, G.; Janes, R. Novel Parallel Integration of Microfluidic Device Network for Emulsion Formation. *Ind. Eng. Chem. Res.* **2009**, *48* (19), 8881–8889. https://doi.org/10.1021/ie900165b.

(22) Muluneh, M.; Issadore, D. Hybrid Soft-Lithography/Laser Machined Microchips for the Parallel Generation of Droplets. *Lab Chip* **2013**, *13* (24), 4750–4754. https://doi.org/10.1039/c3lc50979f.

(23) Jeong, H. H.; Yelleswarapu, V. R.; Yadavali, S.; Issadore, D.; Lee, D. Kilo-Scale Droplet Generation in Three-Dimensional Monolithic Elastomer Device (3D MED). *Lab Chip* **2015**, *15* (23), 4387–4392. https://doi.org/10.1039/c5lc01025j.

(24) Jeong, H. H.; Issadore, D.; Lee, D. Recent Developments in Scale-up of Microfluidic Emulsion Generation via Parallelization. *Korean J. Chem. Eng.* **2016**, *33* (6), 1757–1766. https://doi.org/10.1007/s11814-016-0041-6.

(25) Jeong, H. H.; Yadavali, S.; Issadore, D.; Lee, D. Liter-Scale Production of Uniform Gas Bubbles: Via Parallelization of Flow-Focusing Generators. *Lab Chip* **2017**, *17* (15), 2667–2673. https://doi.org/10.1039/c7lc00295e.

(26) Romanowsky, M. B.; Abate, A. R.; Rotem, A.; Holtze, C.; Weitz, D. A. High Throughput Production of Single Core Double Emulsions in a Parallelized Microfluidic Device. *Lab*

Chip **2012**, *12* (4), 802–807. https://doi.org/10.1039/c2lc21033a.

(27) Yadavali, S.; Jeong, H. H.; Lee, D.; Issadore, D. Silicon and Glass Very Large Scale Microfluidic Droplet Integration for Terascale Generation of Polymer Microparticles. *Nat. Commun.* **2018**, *9* (1), 1-. https://doi.org/10.1038/s41467-018-03515-2.

(28) Femmer, T.; Jans, A.; Eswein, R.; Anwar, N.; Moeller, M.; Wessling, M.; Kuehne, A. J. C. High-Throughput Generation of Emulsions and Microgels in Parallelized Microfluidic Drop-Makers Prepared by Rapid Prototyping. *ACS Appl. Mater. Interfaces* **2015**, *7* (23), 12635–12638. https://doi.org/10.1021/acsami.5b03969.

(29) Tondeur, D.; Luo, L. Design and Scaling Laws of Ramified Distributors by the Constructal Approach. *Chem. Eng. Sci.* **2004**, *59*, 1799–1813. https://doi.org/10.1016/j.ces.2004.01.034.

(30) Luo, L.; Tondeur, D. Optimal Distribution of Viscous Dissipation in a Multi-Scale Branched Fluid Distributor. *Int. J. Therm. Sci.* **2005**, *44*, 1131–1141. https://doi.org/10.1016/j.ijthermalsci.2005.08.012.

(31) Zhu, P.; Wang, L. Passive and Active Droplet Generation with Microfluidics: A Review. *Lab Chip* **2017**, *17* (1), 34–75. https://doi.org/10.1039/C6LC01018K.

(32) Clanet, C.; Lasheras, J. Transition from Dripping to Jetting. *J. Fluid Mech.* **1999**, *383*, 307–326.

(33) Viswanathan, H. Breakup and Coalescence of Drops during Transition from Dripping to Jetting in a Newtonian Fluid. *Int. J. Multiph. Flow* **2019**, *112*, 269–285. https://doi.org/10.1016/j.ijmultiphaseflow.2018.09.016.

(34) Chakraborty, I.; Rubio-Rubio, M.; Sevilla, A.; Gordillo, J. M. Numerical Simulation of Axisymmetric Drop Formation Using a Coupled Level Set and Volume of Fluid Method. *Int. J. Multiph. Flow* **2016**, *84*, 54–65. https://doi.org/10.1016/j.ijmultiphaseflow.2016.04.002.

(35) Utada, A. S.; Fernandez-Nieves, A.; Stone, H. A.; Weitz, D. A. Dripping to Jetting Transitions in Coflowing Liquid Streams. *Phys. Rev. Lett.* **2007**, *99* (9), 1–4. https://doi.org/10.1103/PhysRevLett.99.094502.

(36) Yan, Y.; Guo, D.; Wen, S. Z. Numerical Simulation of Junction Point Pressure during Droplet Formation in a Microfluidic T-Junction. *Chem. Eng. Sci.* **2012**, *84*, 591–601. https://doi.org/10.1016/j.ces.2012.08.055.

(37) Bihi, I.; Vesperini, D.; Kaoui, B.; Le Goff, A. Pressure-Driven Flow Focusing of Two Miscible Liquids. *Phys. Fluids* **2019**, *31* (6). https://doi.org/10.1063/1.5099897.

(38) Bruus, H. *Theorethical Microfluids*; 2008; Vol. 1. https://doi.org/10.1017/CBO9781107415324.004.

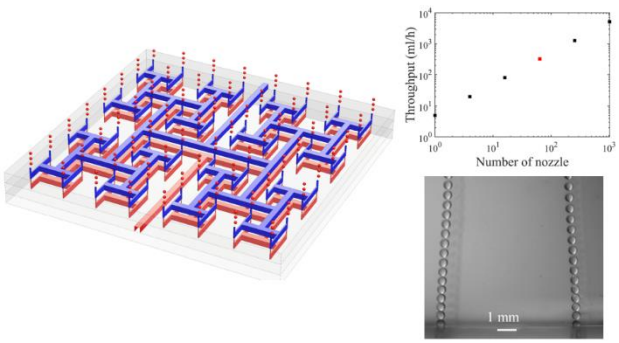

For table of content only